Ga-Doped ZnO Film as a Transparent Electrode for Phthalocyanine/Perylene Heterojunction Solar Cell

Yuki Yoshida, Senku Tanaka[1], Ichiro Hiromitsu[*], Yasuhisa Fujita[2], and Katsumi Yoshino[3,4]

Department of Material Science, Faculty of Science and Engineering, Shimane University, Matsue 690-8504, Japan

[1] *Center for Integrated Research in Science, Shimane University, Matsue 690-8504, Japan*

[2] *Department of Electronic and Control Systems Engineering, Faculty of Science and Engineering, Shimane University, Matsue 690-8504, Japan*

[3] *Collaboration Center, Shimane University, Matsue 690-0816, Japan*

[4] *Center for Advanced Science and Innovation, Osaka University, Suita, Osaka 565-0871, Japan*

[*] E-mail address: hiromitu@riko.shimane-u.ac.jp

Abstract

The photovoltaic properties of Zn-phthalocyanine (ZnPc)/3,4,9,10-perylene-tetracarboxyl -bis-benzimidazole (PTCBI) heterojunction solar cells using Ga-doped ZnO (GZO) film as a transparent electrode are studied. When GZO is the electrode in contact with the donor layer, i.e., ZnPc, the energy conversion efficiency η is only 1/4 of that for the cell using indium-tin-oxide (ITO) as the electrode. When GZO is the electrode in contact with the acceptor layer, i.e., PTCBI, on the other hand, the cell has a three times larger η than the cell using ITO. These results are explained by the work function of GZO being lower than that of ITO. When GZO, or ITO, is used as an electrode for PTCBI, an interesting aging effect is observed. For example, by keeping the GZO-based cell in open air for 6 days in the dark, the energy conversion efficiency and the short-circuit current are increased by factors of 1.67 and 1.36, respectively.

KEYWORDS: solar cells, organic semiconductors, heterojunction, zinc oxide, transparent electrode

1. Introduction

Organic solar cells have been studied as candidates for practical organic-semiconductor-based devices.[1,2] Since the incident light needs to penetrate into the organic layer, one of the electrodes of the solar cell should be transparent. The most widely used transparent electrode is indium-tin-oxide (ITO) film because of its high transmissivity for visible light and low sheet resistance. Usually, ITO is used as an anode because of its relatively high work function. Many types of organic solar cells with ITO electrodes have been reported.[3,4] However, ITO has the following problems: 1) The price of ITO has been rising markedly in recent years. 2) ITO forms a weak blocking contact with an n-type, (acceptor), layer, while it forms a good electrical contact with a p-type, (donor), layer. Therefore, finding other materials suitable for the transparent electrode is an important subject.[5-7] One of the candidates is ZnO, which is a II-VI compound semiconductor with a wurtzite structure. ZnO has a band gap of 3.4 eV.[8] Therefore, ZnO is transparent for visible light. Furthermore, the conductivity of ZnO can be increased by n-type doping.[9,10] Several organic solar cells using ZnO have been reported, e.g., heterojunctions[11-13] and bulk heterojunctions[12,14] using ZnO as a transparent electrode, and a bulk heterojunction using ZnO nanoparticles.[15]

In this paper, Zn-phthalocyanine (ZnPc)/3,4,9,10-perylene-tetracarboxyl-bis -benzimidazole (PTCBI) heterojunction solar cells using a Ga-doped ZnO (GZO) film as a

transparent electrode are reported, in which ZnPc and PTCBI are typical organic semiconductors for solar cells[3,16] having electron-donating and -accepting properties, respectively. The GZO film has a high optical transmissivity and a low sheet resistance, which are comparable to those of ITO. GZO has an advantage against ITO because Ga and Zn are more abundant in the earth's crust than In (Ga: 18 ppm, Zn: 80 ppm, In: 0.05 ppm)[17] and, as a result, GZO is cheaper than ITO. It will be shown that GZO gives better photovoltaic characteristics than ITO when it is used as an electrode for the acceptor, i.e., PTCBI. An interesting aging effect of the device will also be reported.

2. Experiment

ZnPc and pentacene were purchased from Kanto Chemical and Aldrich, respectively. PTCBI was synthesized by a literature-based procedure.[18] These chemicals were used after three sublimations in vacuum. ITO substrates of 50 Ω/sq. sheet resistance were purchased from Geomatec.

GZO films were deposited on quartz substrates (9×24×1 mm^3) by RF magnetron sputtering from a GZO ceramic target with a Ga content of 5.7 wt% purchased from AGC Ceramics. The substrate temperature during the deposition was 300°C. The film thickness of the GZO film was estimated to be ~200 nm from the interference peaks in the optical absorption spectrum. The sheet resistance was 35 Ω/sq., and the transmissivity for visible

light was over ~90%.

Three types of heterojunction cells were prepared, the schemes of which are shown in Fig. 1, and the molecular structures of ZnPc, PTCBI, and pentacene are shown in Fig. 2. In type A, GZO or ITO was used as an electrode for ZnPc, while, in types B and C, it was used as an electrode for PTCBI. In type A, the Al film is a supporting electrode for In because the conductivity of In is quite poor. In type B, the film thickness of the ZnPc film was chosen to be relatively large in order to prevent a short-circuit failure due to the penetration of Au particles. In type C, the pentacene layer was intercalated between the ZnPc and Au layers as a buffer layer to prevent the short-circuit failure. All the films except GZO and ITO were prepared by vacuum evaporation under a pressure of 1×10^{-4} Pa. The speeds of evaporation were 0.1 nm/s for PTCBI, ZnPc, and pentacene, 0.05 nm/s for In and Al, and 0.01 nm/s for Au, as monitored using a quartz oscillator (ULVAC CRTM-5000 or CRTM-6000). The active area of the device was 0.3 cm^2.

The electrical circuit for current-voltage measurement is shown in Fig. 1. The positive directions of the current, I, and the applied bias voltage, V_{bias}, are defined for the device of each type in Fig. 1, which correspond to the forward bias direction. The current, I, was measured from the voltage drop across a small resistance, r. The photocurrent measurement was carried out under an illumination of 100 mW/cm^2 light with an AM 1.5 spectrum, which was obtained using a 300 W Xe lamp followed by homemade optical filters having an

appropriate absorption spectrum. All measurements were carried out in vacuum at room temperature.

3. Results

3.1 Type A: (GZO or ITO)/ZnPc/PTCBI/In/Al

Figure 3(a) shows the bias dependence of the dark current density, J_{dark}, of the cells of type A in which GZO or ITO is used as an electrode for the ZnPc layer. Immediately after the device preparation, the rectification ratios at $V_{bias} = \pm 2$ V were 3.7 and 137 for the cells using GZO and ITO, respectively. After keeping the cells in Ar gas for 8 or 11 days in the dark, the rectification ratios were degraded to 2.3 and 8.2 for the two cells, respectively. Figure 3(b) shows the bias dependence of the photocurrent density, J_{photo}, of these cells. Immediately after the device preparation, the short-circuit current density J_{sc}, open-circuit voltage V_{oc}, and the energy conversion efficiency η were 0.80 mA/cm^2, 0.25 V, and 0.05% for the GZO-based cell, and 1.86 mA/cm^2, 0.43 V, and 0.20% for the ITO-based cell, respectively. After keeping the cells in Ar gas for 8 or 11 days in the dark, the photovoltaic properties were degraded to J_{sc} = 0.29 mA/cm^2, V_{oc} = 0.20 V, and η = 0.01% for the GZO-based cell, and J_{sc} = 0.71 mA/cm^2, V_{oc} = 0.40 V, and η = 0.06% for the ITO-based cell. A similar degradation was observed when the device was kept in open air instead of Ar gas. Comparing the GZO- and ITO-based cells, we can observe that the former has poorer rectification and photovoltaic properties both

before and after the degradation.

3.2 Type B: (GZO or ITO)/PTCBI/ZnPc/Au

Figure 4(a) shows the bias dependence of the J_{dark} of the cells of type B in which GZO or ITO is used as an electrode for the PTCBI layer. The thickness of the ZnPc layer was chosen to be 150 nm in order to prevent the short-circuit failure due to the penetration of Au particles into the organic layer. Immediately after the device preparation, the rectification ratios at V_{bias} = ±2 V were 11 and 23 for the cells using GZO and ITO, respectively. After keeping the cells in open air for 63 days in the dark, the rectification ratios of the two cells were increased to 180 and 567, respectively. Figure 4(b) shows the bias dependence of the J_{photo} of these cells. Immediately after the device preparation, J_{sc}, V_{oc}, and η were 0.44 mA/cm^2, 0.30 V, and 0.03% for the GZO-based cell, and 0.25 mA/cm^2, 0.35 V, and 0.02% for the ITO-based cell, respectively. After keeping the cells in open air for 63 days in the dark, J_{sc}, V_{oc}, and η were improved to 1.26 mA/cm^2, 0.46 V, and 0.17% for the GZO-based cell, and 1.03 mA/cm^2, 0.45 V, and 0.11% for the ITO-based cell, respectively. Comparing the GZO- and ITO-based cells, we can observe that the former has better photovoltaic properties both before and after aging while the ITO-based cell shows a higher rectification ratio. The J_{sc} and η of the cells of type B are not satisfactorily high because of a large series resistance coming from the thick ZnPc layer.

3.3 Type C: (GZO or ITO)/PTCBI/ZnPc/pentacene/Au

To reduce the series resistance, the cells of type C were prepared in which a pentacene buffer layer was intercalated between the ZnPc and Au layers instead of using a thick ZnPc layer. Figure 5(a) shows the bias dependence of the J_{dark} of the cells of type C. Immediately after the device preparation, the rectification ratios at $V_{bias} = \pm 2$ V were 686 and 171 for the cells using GZO and ITO, respectively. After keeping the cells in open air for 58 days with no illumination, the rectification ratios of the two cells were increased to 7113 and 595, respectively. Figure 5(b) shows the bias dependence of the J_{photo} of these cells. Immediately after the device preparation, J_{sc}, V_{oc}, and η were 1.03 mA/cm^2, 0.45 V, and 0.10% for the GZO-based cell, and 0.51 mA/cm^2, 0.35 V, and 0.03% for the ITO-based cell, respectively. After keeping the cells in open air for 58 days in the dark, the photovoltaic properties were improved to J_{sc} = 1.28 mA/cm^2, V_{oc} = 0.48 V, and η = 0.19% for the GZO-based cell, and J_{sc} = 0.87 mA/cm^2, V_{oc} = 0.40 V and η = 0.08% for the ITO-based cell. Comparing the GZO- and ITO-based cells, we can observe that the former has much better rectification and photovoltaic properties both before and after aging.

Figure 6(a) shows the photocurrent action spectra of the GZO-based cell of type C with V_{bias} = 0 V for the two illumination directions from the GZO and Au sides. Comparing the action spectra in Fig. 6(a) with the optical absorption spectra of ZnPc, PTCBI, and pentacene

films in Fig. 6(b), it is seen that the photocurrent is generated by the optical excitations of ZnPc and PTCBI. The excitation of pentacene does not contribute to the photocurrent generation, which is clearly seen in the action spectrum with the illumination from the Au side by the lack of the corresponding peaks in the wavelength range between 620 and 700 nm. Thus, the pentacene layer works purely as a buffer layer, that prevents the penetration of Au particles into the ZnPc layer. Comparing the cells of types B and C, we can observe that the latter shows higher J_{sc} and η before aging, which is attributed to the resistance of the pentacene film being lower than that of the ZnPc film, while, after the aging in open air, the cells of types B and C show similar photovoltaic characteristics, which may be attributed to an oxygen doping of the ZnPc and pentacene layers, which may make the resistivities of the two layers similar.

3.4 Atmosphere dependence of the aging effect

One of the interesting results in Figs. 4 and 5 is the improvement of the photovoltaic characteristics after keeping the cells of types B and C in open air. The atmosphere dependence of the aging effect was studied for the GZO-based cell of type C. Figure 7 shows the time dependences of the η, J_{sc}, fill factor FF, and V_{oc} of the cell in three types of atmosphere, i.e., in open air, in Ar gas of 1 atm pressure, and in vacuum. In the experiment, the cell was kept in the dark, and the measurement was carried out every 2 days. In open air,

all the four quantities were increased by aging. In particular, η and J_{sc} were increased by factors of 1.67 and 1.36, respectively, after 6 days. In Ar gas, all the quantities showed only a small change. In vacuum, η and J_{sc} were decreased to values that were 0.78- and 0.89-fold the initial values, respectively, after aging for 6 days, although FF and V_{oc} varied in a complicated manner. Thus, the improvement of the photovoltaic properties brought about by aging was observed only in open air. A possible explanation may be that an oxygen doping of the ZnPc and pentacene layers takes place during the aging, which may result in a reduction of the series resistance of the cell. The increase in the dark current under forward bias in Fig. 5(a) supports this explanation. In the case of the cells of type A, the oxygen doping of the ZnPc layer may not have occurred efficiently because the ZnPc layer is covered by the PTCBI layer. The origin of the degradation of the cells of type A by the aging in Ar gas or in open air is unknown at present.

4. Discussion

4.1 Origin of the difference between GZO- and ITO-based cells

In the present results, the GZO-based cell had better rectification and photovoltaic characteristics than the ITO-based cell for type C, while the ITO-based cell had better characteristics than the GZO-based cell for type A. A similar result has been reported by Owen *et al.* for a bulk heterojunction solar cell.[14)] These results are explained by a difference

in the work function, Φ, between GZO and ITO. The Fermi level of GZO is assumed to coincide with the conduction-band edge because the present GZO film is highly conductive due to the n-type doping with Ga. Then, the Φ of GZO is obtained by the following relationship.

$$\Phi \text{ of GZO} \approx (\text{Ionization potential: } IP) - (\text{Band gap: } E_g) \quad (1)$$

IP was estimated to be 7.8 eV by ultraviolet photoelectron spectroscopy, and E_g was estimated to be 3.4 eV by optical absorption. Thus, the Φ of GZO is estimated to be 4.4 eV. On the other hand, the typical value of Φ reported for ITO is 4.7 eV.[19)]

Figure 8 shows the energy band diagrams of the cells of type C before and after the junctions are made. For the cells of type C, the fact that the rectification ratio of the GZO-based cell is larger than that of the ITO-based cell is a result of the larger forward current of the GZO-based cell. The larger forward current is attributable to the smaller electron injection barrier at the electrode/PTCBI interface for the GZO-based cell. The better photovoltaic properties of the GZO-based cell, on the other hand, are attributed to a larger electric field in the organic layers, which is a result of the smaller Φ for GZO. In Fig. 8(b), the slope of the energy band is proportional to the internal electric field. Since the work-function difference between GZO and Au is larger than that between ITO and Au, the electric fields in the PTCBI and ZnPc layers are expected to become larger for the GZO-based cell, as shown in Fig. 8(b), due to the Fermi-level alignment through the device. The larger electric field

causes a larger carrier-generation efficiency[16,20-22] as well as a higher carrier drift velocity.

The results for the cells of type A can be explained in a similar manner. For the cells of type B, on the other hand, the GZO-based cell had a lower rectification ratio than the ITO-based cell, which was a result of a larger reverse current for the GZO-based cell. The reverse current of the cells of type B may be determined by the leakage current due to the penetration of the Au particles into the organic layers, which may not be well controlled in the present device preparation of type B.

4.2 Aging effect

In the present experiment, the rectification and photovoltaic properties of the cells of types B and C were improved by aging in open air, while those of the cells of type A were degraded by the aging. Owen *et al.* reported an aging effect for GZO-based bulk heterojunction cells with a GZO/poly 3-hexylthiophene (P3HT):[6,6]-phenyl-C_{61}-butyric acid methyl ester (PCBM)/ poly(ethylenedioxy) thiophene:poly(styrene) sulfonate (PEDOT:PSS)/Au structure.[14] In this case, the degradation of the photovoltaic characteristics is prevented by an encapsulation of the photocurrent active layer P3HT:PCBM under the PEDOT:PSS layer. In Owen's system, the introduction of air into the active layer causes a degradation, while, in the present systems of types B and C, it improves the device characteristics. The difference may be attributed to the difference in the device structure. In the bulk heterojunction, the air

molecules can easily reach the acceptor phase, which may reduce the photovoltaic activity of the acceptor, while, in the present heterojunctions of types B and C, the penetration of air molecules into the acceptor layer is blocked by the ZnPc layer.

5. Conclusions

The GZO-based cells of types B and C showed significantly better photovoltaic properties than the ITO-based cells, while the photovoltaic properties of the GZO-based cell of type A was not as good as those of the ITO-based cell. This indicates that GZO can be used as a good transparent electrode in contact with the acceptor layer. The experimental results can be explained by the work function of GZO being smaller than that of ITO.

The photovoltaic properties of the cells of types B and C were improved by keeping the cells in open air with no illumination. For example, the η and J_{sc} of the GZO-based cell of type C were increased by factors of 1.67 and 1.36, respectively, after an aging of 6 days. This effect may be explained by the p-type doping of ZnPc and pentacene layers due to the penetration of oxygen molecules into these donor layers.

References

1. C. J. Brabec, N. S. Sariciftci, and J. C. Hummelen: Adv. Funct. Mater. **11** (2001) 15.
2. H. Spanggaard and F. C. Krebs: Sol. Energy Mater. Sol. Cells **83** (2004) 125.
3. C. W. Tang: Appl. Phys. Lett. **48** (1986) 183.
4. T. Yamanari, T. Taima, K. Hara, and K. Saito: J. Photochem. Photobiol. A **182** (2006) 269.
5. R. Ulbricht, X. Jiang, S. Lee, K. Inoue, M. Zhang, S. Fang, R. Baughman, and A. Zakhidov: Phys. Status Solidi B **243** (2006) 3528.
6. B. Winther-Jensen and F. C. Krebs: Sol. Energy Mater. Sol. Cells **90** (2006) 123.
7. T. Ootsuka, Z. Liu, M. Osamura, Y. Fukuzawa, R. Kuroda, Y. Suzuki, N. Otogawa, T. Mise, S. Wang, Y. Hoshino, Y. Nakayama, H. Tanoue, and Y. Makita: Thin Solid Films **476** (2005) 30.
8. S. J. Pearton, D. P. Norton, K. Ip, Y. W. Heo, and T. Steiner: Prog. Mater. Sci. **50** (2005) 293.
9. J. Han, P. Q. Mantas, and A. M. R. Senos: J. Eur. Ceram. Soc. **21** (2001) 1883.
10. Z. Zhou, K. Kato, T. Komaki, M. Yoshino, H. Yukawa, M. Morinaga, and K. Morita: J. Eur. Ceram. Soc. **24** (2004) 139.
11. T. Shirakawa, T. Umeda, Y. Hashimoto, A. Fujii, and K. Yoshino: J. Phys. D **37** (2004)

847.

12. T. Umeda, T. Shirakawa, A. Fujii, and K. Yoshino: Jpn. J. Appl. Phys. **42** (2003) L1475.
13. J. C. Bernède, H. Derouiche, and V. Djara: Sol. Energy Mater. Sol. Cells **87** (2005) 261.
14. J. Owen, M. S. Son, K.-H. Yoo, B. D. Ahn, and S. Y. Lee: Appl. Phys. Lett. **90** (2007) 033512.
15. G. D. Sharma, R. Kumar, S. K. Sharma, and M. S. Roy: Sol. Energy Mater. Sol. Cells **90** (2006) 933.
16. I. Hiromitsu, Y. Murakami, and T. Ito: J. Appl. Phys. **94** (2003) 2434.
17. *Rika Nenpyo 2007* (Chronological Scientific Tables) ed. National Astronomical Observatory (Maruzen, Tokyo, 2006) Chap. 5 [in Japanese].
18. T. Maki and H. Hashimoto: Bull. Chem. Soc. Jpn. **25** (1952) 411.
19. J. A. Chaney and P. E. Pehrsson: Appl. Surf. Sci. **180** (2001) 214.
20. I. Hiromitsu and G. Kinugawa: Jpn. J. Appl. Phys. **44** (2005) 60.
21. Y. Yoshida, M. Nakamura, S. Tanaka, I. Hiromitsu, Y. Fujita, and K. Yoshino: Synth. Met. **156** (2006) 1213.
22. I. Hiromitsu, S. Mada, A. Inoue, Y. Yoshida, and S. Tanaka: Jpn. J. Appl. Phys. **46** (2007) 7241.

Captions

Fig. 1. Schemes of three types of ZnPc/PTCBI heterojunction cells studied, and the electric circuit for current-voltage measurement.

Fig. 2. Molecular structures of the organic substances used in the present study.

Fig. 3. Bias dependence of the current density of the cells of type A. (a) In the dark. (b) Under illumination. The illumination was from the transparent electrode, with an AM 1.5 light of 100 mW/cm^2.

Fig. 4. Bias dependence of the current density of the cells of type B. (a) In the dark. (b) Under illumination. The illumination was from the transparent electrode, with an AM 1.5 light of 100 mW/cm^2.

Fig. 5. Bias dependence of the current density of the cells of type C. (a) In the dark. (b) Under illumination. The illumination was from the transparent electrode, with an AM 1.5 light of 100 mW/cm^2.

Fig 6. (a) Photocurrent action spectra of the GZO-based cell of type C under the

short-circuit condition with illuminations from the GZO and Au sides. The current for the illumination from the Au side was enlarged by a factor of 4. (b) The optical absorption spectra of ZnPc, PTCBI, and pentacene films.

Fig. 7. Effect of aging of the GZO-based cell of type C under three kinds of atmosphere, i.e., in open air, in Ar gas, and in vacuum, on (a) energy conversion efficiency η, (b) short-circuit current density J_{sc}, (c) fill factor FF, and (d) open-circuit voltage V_{oc}.

Fig. 8. Energy band diagrams for the GZO-based cell of type C (a) before and (b) after the junctions were made. $V_{bias} = 0$ V.

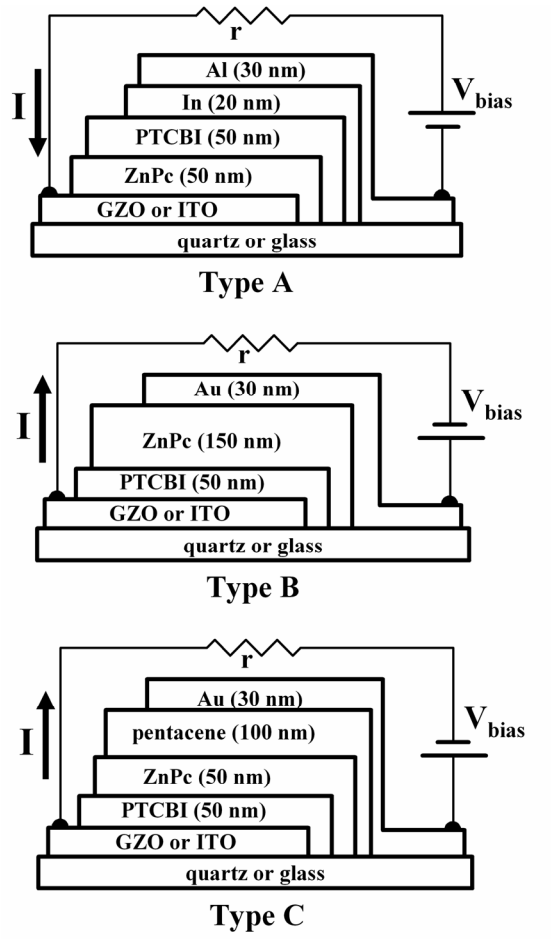

Fig. 1 Y. Yoshida et al.

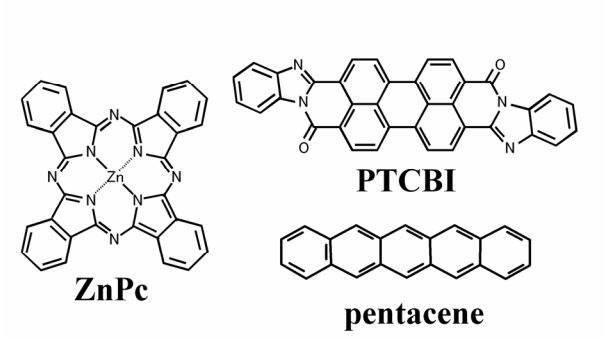

Fig. 2 Y. Yoshida et al.

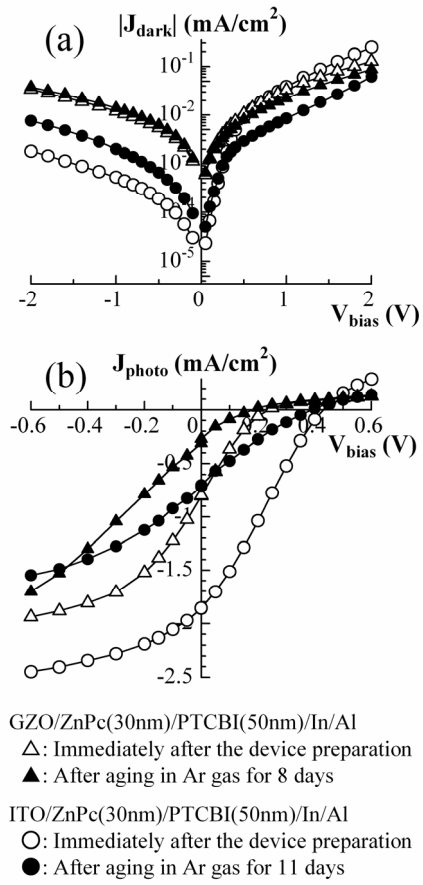

Fig. 3 Y. Yoshida et al.

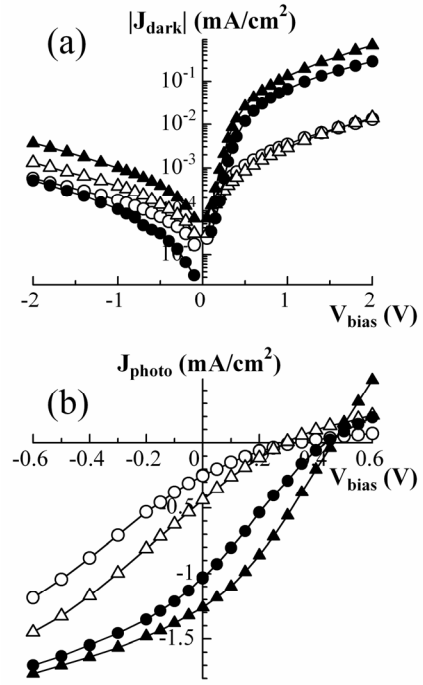

GZO/PTCBI(50nm)/ZnPc(150nm)/Au
△: Immediately after the device preparation
▲: After aging in the air for 63 days

ITO/PTCBI(50nm)/ZnPc(150nm)/Au
○: Immediately after the device preparation
●: After aging in the air for 63 days

Fig. 4 Y. Yoshida et al.

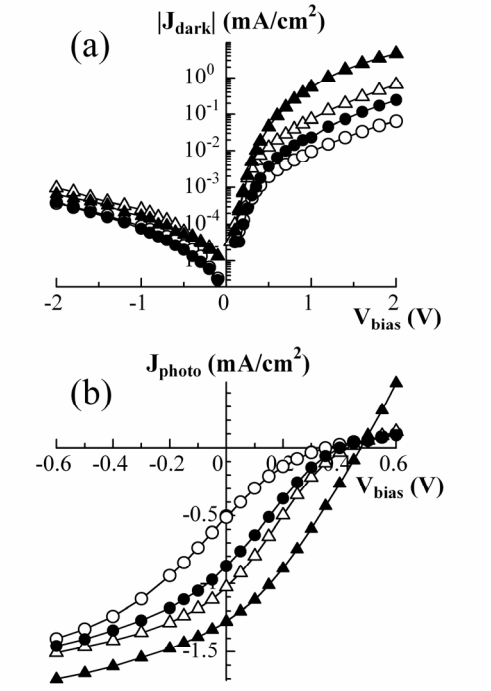

GZO/PTCBI(50nm)/ZnPc(50nm)/pentacene(100)/Au
△: Immediately after the device preparation
▲: After aging in the air for 58 days

ITO/PTCBI(50nm)/ZnPc(50nm)/pentacene(100)/Au
○: Immediately after the device preparation
●: After aging in the air for 58 days

Fig. 5 Y. Yoshida et al.

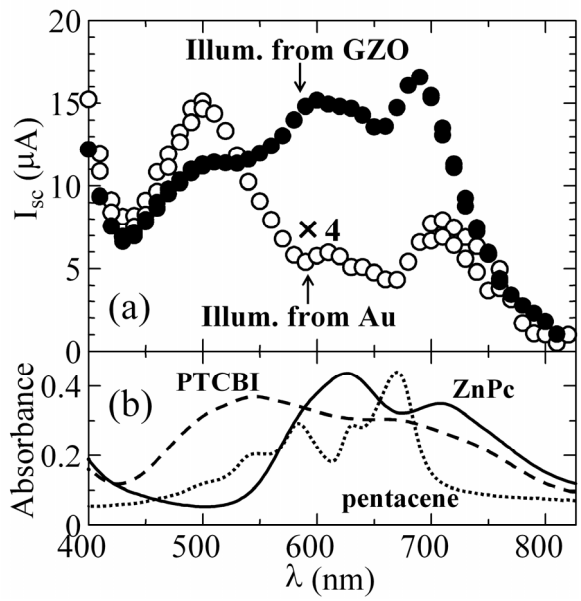

Fig. 6 Y. Yoshida et al.

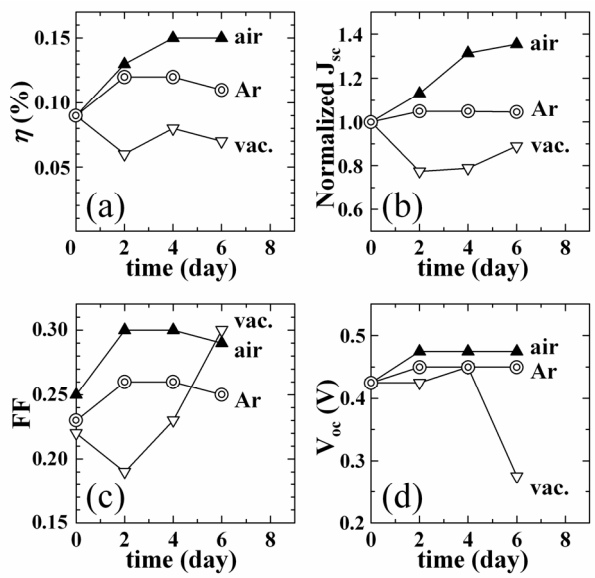

Fig. 7 Y. Yoshida et al.

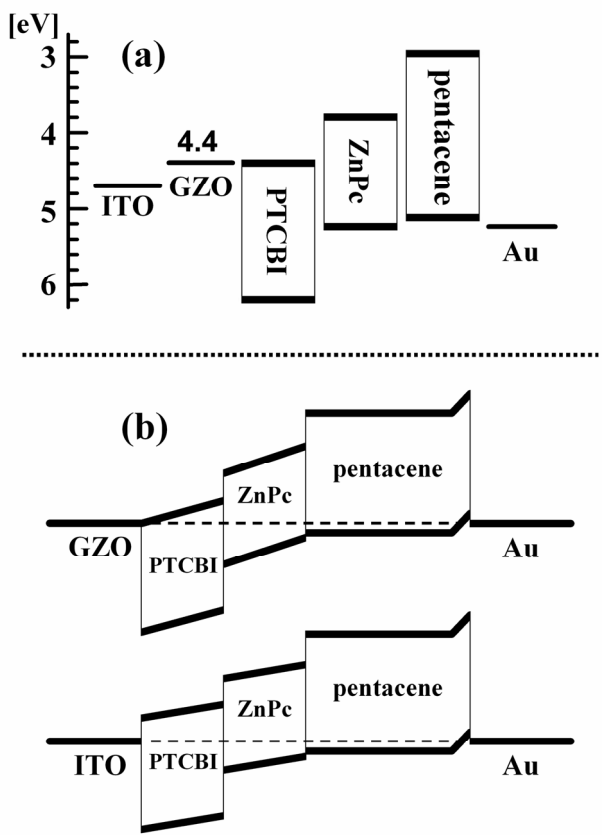

Fig. 8 Y. Yoshida et al.